Fatigue damage monitoring and evolution for basalt fiber reinforced polymer materials

Hui Li[*], Wentao Wang[a] and Wensong Zhou[b]

Research Center of Structural Monitoring and Control, School of Civil Engineering, Harbin Institute of Technology, Harbin 150090, China

Abstract. A newly developed method based on energy is presented to study the damage pattern of FRP material. Basalt fiber reinforced polymer (BFRP) is employed to monitor the damage under fatigue loading. In this study, acoustic emission technique (AE) combined with scanning electronic microscope (SEM) technique is employed to monitor the damage evolution of the BFRP specimen in an approximate continuous scanning way. The AE signals are analyzed based on the wavelet transform, and the analyses are confirmed by SEM images. Several damage patterns of BFRP material, such as matrix cracking, delamination, fiber fracture and their combinations, are identified through the experiment. According to the results, the cumulative energy (obtained from wavelet coefficients) of various damage patterns are closely related to the damage evolution of the BFRP specimens during the entire fatigue tests. It has been found that the proposed technique can effectively distinguish different damage patterns of FRP materials and describe the fatigue damage evolution.

Keywords: fatigue damage; acoustic emission; wavelet transform; damage pattern; damage evolution

1. Introduction

Nowadays, fiber reinforced polymer (FRP) material is extensively used in many areas, such as aerospace engineering, mechanical engineering, civil engineering and medical science due to its superior mechanical properties, excellent physical and chemical performance. Especially in civil engineering, FRP is an ideal structural material used in civil buildings and bridges. Basalt fiber reinforced polymer (BFRP) is a type of FRP which is widely used in some structures in China. Its fibers are made from basalt rock. Basalt fiber has good range of thermal performance, high tensile strength, resistance to acids, good electro-magnetic properties, inert nature, and resistance to corrosion, vibration and impact loading. Furthermore, BFRP products are available in a variety of forms such as, plates, straight rods and loops.

In civil engineering, BFRP can also be used to retrofit or strengthen existing structure by wrapping or attaching it on the surface of structural elements. In order to ensure the safety of composites structures during their lifetimes, it is imperative to monitor, analyze and evaluate the

---

∗Corresponding author, Professor, E-mail: lihui@hit.edu.cn
[a] Ph.D. Student, E-mail: wentaowang@hit.edu.cn
[b] Associate Professor, E-mail: zhouwensong@hit.edu.cn

various damage patterns caused by both static and dynamic loads and by environmental effects (Eckles and Awerbuch 1988, Fang and Berkovits 1995).

Recently, many of these non-destructive tests involve the periodic inspection of composite components by means of costly equipments. There is thus a growing interest in the development of smart structures which integrate sensors allowing the in situ monitoring of damage throughout life. Optical fibers and other sensors, such as piezoelectric transformers, are suggested smart sensing constituents for damage monitoring of FRP. Compared with optical fiber sensor, piezoelectric transformers can catch the acoustic emission signals during the damage of FRP, which contains plenty of information about the damage procedure (Maji *et al.* 1997, Giordano *et al.* 1998, Caprino *et al.* 2005, Park *et al.* 2007, de Oliveira and Marques 2008, Park *et al.* 2008). There is a large volume of research on damage detection techniques for FRP materials through the acoustic emission technique. To name a few, unidirectional composites are tested under different loading conditions (de Groot *et al.* 1995, Surgeon and Wevers 1999, Mizutani *et al.* 2000, Gutkin *et al.* 2011). As above stated, the AE signals generated at fracture of composites could be related to the damage patterns and mechanism during kinds of mechanical tests such as static, impact and fatigue. Indicator derived from frequency, amplitude, energy and the other conventional AE parameters can be used to determine the failure of the composites (Philippidis and Assimakopoulou 2008, Unnthorsson *et al.* 2008, Gutkin *et al.* 2011). It is worth noting that the frequencies of AE signals are almost unchanged, while, the amplitudes (or energies) attenuate greatly with the increment of propagation length. This prove that the frequency analysis is an effective way in processing AE signals of composite materials (Ni and Iwamoto 2002). In order to obtain the frequency characteristics of AE signals of FRP materials, peak frequency analysis (Gutkin *et al.* 2011) and wavelet transform are two of the most widely used methods. For the analysis of the frequency content of AE signals from FRP composites, some studies shows very successful results for the relationship between the damage patterns and frequencies. Based on the research achievements of predecessors, several specific damage patterns of FRP materials are obtained: matrix cracking, delamination, fiber pull-out and fiber fracture (de Groot *et al.* 1995, Qi 2000, Sung *et al.* 2002, Ding *et al.* 2004, Sohn *et al.* 2004, Grabowska *et al.* 2008). However, it should be noted that their investigation lacked information on microscopic observations from SEM or optical microscopy. The detailed microstructure images are very useful to the researches of FRP materials.

The present investigation is aimed at correlating AE signals with fracture phenomena of the BFRP specimens. AE signals are acquired by piezoelectric sensor, which can be attached on the surface of specimens with small size instead of conventional AE sensors. With the proposed configuration in this work, it is possible to implement continuous scanning electronic microscopy test on the small specimen in the process. The fracture phenomena can be observed from the scanning electronic microscopy.

This paper focuses on the damage patterns and damage evolution of BFRP material. In section 2, three-point bending fatigue experiments are designed and performed. Acoustic emission technique and SEM are proposed to monitor the damage simultaneously. With the proposed configuration in this work, it is possible to implement continuous scanning electronic microscopy test on the small specimen in the process. The data analysis and signal processing portion of this study is described in the following sections. The method based on wavelet transform is employed to analyze the characteristics of AE signals instead of the traditional peak frequency method. In section 4, experimental results and further analysis are described in detail. In section 5, three basic damage patterns are obtained through previous analyses. Furthermore, the fatigue damage

evolution of BFRP material can be described by cumulative energy. Conclusions and scope of future work are presented in the last section.

2. Experiment

In this study, the tensile test and bending test of FRP plates under monotonically increasing loading are first conducted to obtain the basic mechanical properties, which will be used to select the appropriate governing parameters in the fatigue stage. Then, the fatigue test is conducted, and the AE system combined with SEM is employed to monitor the accumulated damage evolution process.

2.1 Materials and BFRP plates

Basalt fiber with a diameter of $7-8\mu m$ which made from basalt rock is employed to fabricate the fiber reinforced polymer (BFRP) in this test. Epoxy resin is used as the matrix of BFRP. The BFRP laminate plate with a size of 25 × 25 cm is produced by the hand lay-up method. The BFRP laminate plate contains 14 layers, and all fibers are unidirectional. To ensure the homogeneous mechanical properties of all specimens, all the test specimens are cut from a same BFRP laminate plate.

2.2 Three-point static loading tests

The three-point static loading tests of the BFRP plates are conducted with the Instron 4505 servo-hydraulic testing machine at the Harbin University of Engineering. A total of 3 specimens (30 mm × 10 mm × 3.8 mm) are tested for this study to determine the ultimate strength of a BFRP laminate plate. The effectiveness span of the specimen is 20 mm. These tests are conducted using the displacement loading control method, and the loading rate is 1 mm/min until failure. The loading and displacement are measured by the loading system. The load-displacement curves from Fig. 1 show that the mean value of the failure load is 1893.88 N and the average bending deflection of the three specimens is 0.798 mm. These results are then used to select the appropriate parameter values to design the three-point loading fatigue tests.
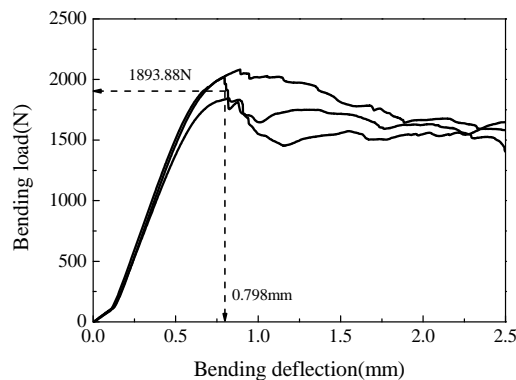

Fig. 1 Three-point bending load deflection curves

2.3 Fatigue test

A total of 2 specimens which are cut from the same BFRP plate are tested for the three-point loading fatigue experiment. As shown in Fig. 2, the size of the BFRP specimen is 50 (length) × 10 (width) × 3.8 mm (thickness), and the effective span is 20 mm.

Three-point loading fatigue tests of the BFRP laminate plates are conducted to investigate the fatigue damage process of BFRP plates. The AE signals are detected by the PZT patch, which acts as an acoustic sensor. To verify the signals collected by the AE system, a scanning electron microscope (SEM) is employed to monitor the damage evolution in the microstructure of the BFRP plate during the fatigue test.

All the fatigue tests are conducted in the State Key Laboratory of Coal Resources and Safe Mining, China University of Mining and Technology (Beijing). The fatigue test instrumentation in this laboratory include the fatigue loading machine and SEM equipment (JEOL 5410LV). This whole system can simultaneously perform the fatigue loading test and SEM observation. The maximum load of the fatigue test machine is 10 kN, its maximum stroke is 25 mm, and its load frequency range is 10^{-5} to 100 Hz. The observation accuracy of the SEM system is 3.5 nm. The combined fatigue and SEM test system are shown in Fig. 3. It should be noted that the SEM can only work in a vacuum chamber. Thus, the images of BFRP plates are actually not continuous. Additionally, it is worth noting that an SEM can only observe changes in the microstructure of the specimen surface instead of the inner damage status.
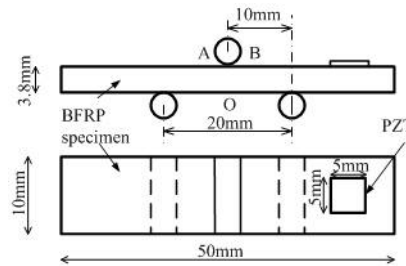

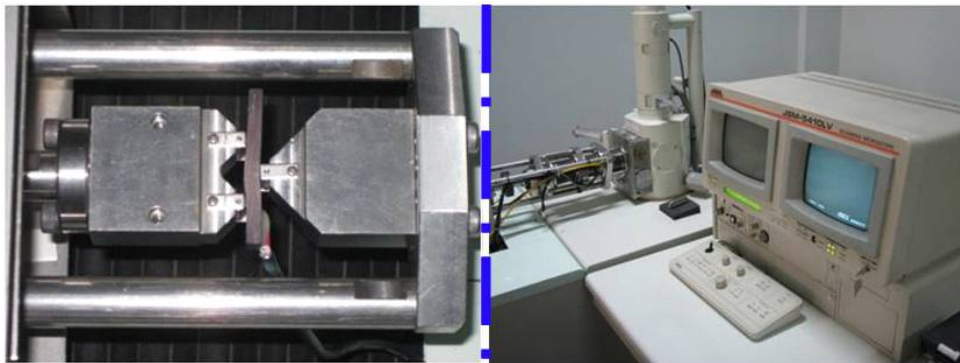Fig. 2 BFRP specimen, the location of the PZT patch

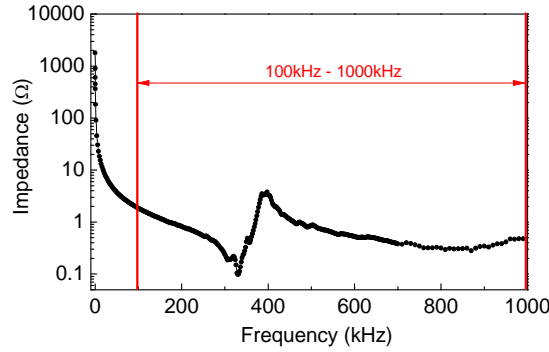Fig. 3 Fatigue loading test set up and SEM test system

Fig. 4 Impedance-frequency curve of the PZT patch

Because the vacuum chamber is very small, traditional acoustic emission sensor cannot be utilized in this test. Therefore, a small square (5 mm×5 mm×0.4 mm) PZT patch is chose to be attached on the free surface of the BFRP layer to form a AE sensor. Additionally, in this study, the PZT patch is covered with conductive adhesive tape to shield against electromagnetic interference. The DiSP system from the Physical Acoustic Corporation is used as the AE signal acquisition instrument. The DiSP system includes a 4-Channel PCI/DSP-4 board and four preamplifiers (100 kHz-1 MHz). The wide-band analog filter has a frequency range of 100 kHz to 400 kHz, and the gain of the preamplifier is 40 dB. The sampling frequency of AE system is 1 MHz. The threshold of the acoustic emission equipment was set to 5 mV, which is a sensitive threshold comparing to the previous studies. Before the fatigue loading test, the impedance of the PZT patch is investigated experimentally. The piezoelectric coefficient of the PZT patch used is $d_{33} = 450 \times 10^{-12}$ C/N, and the compliance coefficients are $s_{11}^E = 17.6 \times 10^{-12}$ m²/N and $s_{33}^E = 19.2 \times 10^{-12}$ m²/N, respectively. The impedance-frequency curve of the PZT patch is shown in Fig. 4. The result indicates that the impedance of PZT is lower than that the data acquisition equipment. Therefore, this PZT patch can work well throughout the test process and obtain accurate voltage.

In this paper, we focus on the damage mechanism of BFRP material. Therefore, too many loading cycles is not so much necessary. In order to reduce the loading cycles the loading amplitude is designed to 700 N and the stress ratio is 0.6. The loading frequency is 2 Hz.

During the experiment, we built a real-time monitoring system. The fatigue damage of FRP material under loading test will cause both the damage inside and the surface damage. The AE signals which present the damage can be received by the equipment. The surface damage can be directly observed by the scanning electronic microscope. Therefore, combining both the AE technique and SEM, we can build a real-time monitoring system. The monitoring scheme follows the designed steps: AE equipment is used to receive the damage signals of specimen until the displacement reaches the pre-specified target (for instance, 0.9 mm, 1.2 mm and 1.5 mm). Then the fatigue loading test is interrupted, and SEM is employed to record the microstructure image. This process will be repeated 6 times (interrupted at the end of each stage for SEM observation) until the specimen fails. The 6 stages are shown in Table 1.

Table 1 The six stages of loading scheme

Stage number	Displacement at mid-span
1	0-0.9 mm
2	0.9-1.2 mm
3	1.2-1.5 mm
4	1.5-1.8 mm
5	1.8-2.1 mm
6	2.1-2.5 mm

3. Wavelet transform and time-frequency analysis

The peak frequency method is frequently used to analyze AE signals. This method finds the maximum peak in a frequency spectrum and ignores others. This method can be used for the AE signal which has just one single frequency component, as the gray curve shown in Fig. 5. However, if an AE signal contains multiple frequency peaks (black curve in Fig. 5), the peak frequency method may lose the useful features of the signals. Therefore, another method is needed to analyze the multiple frequency components of AE signals.
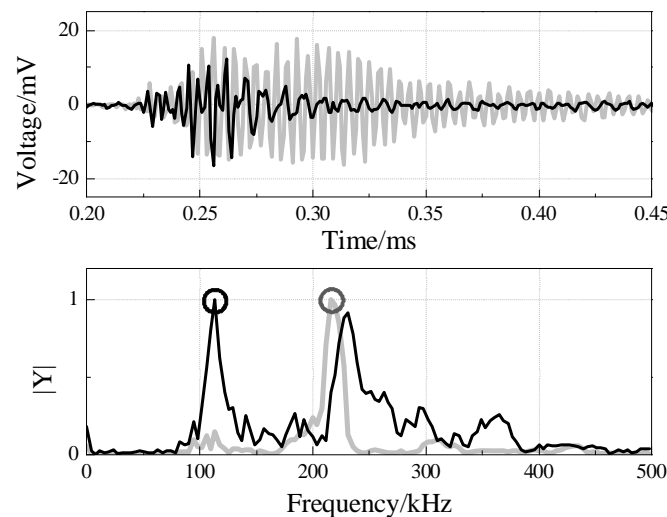

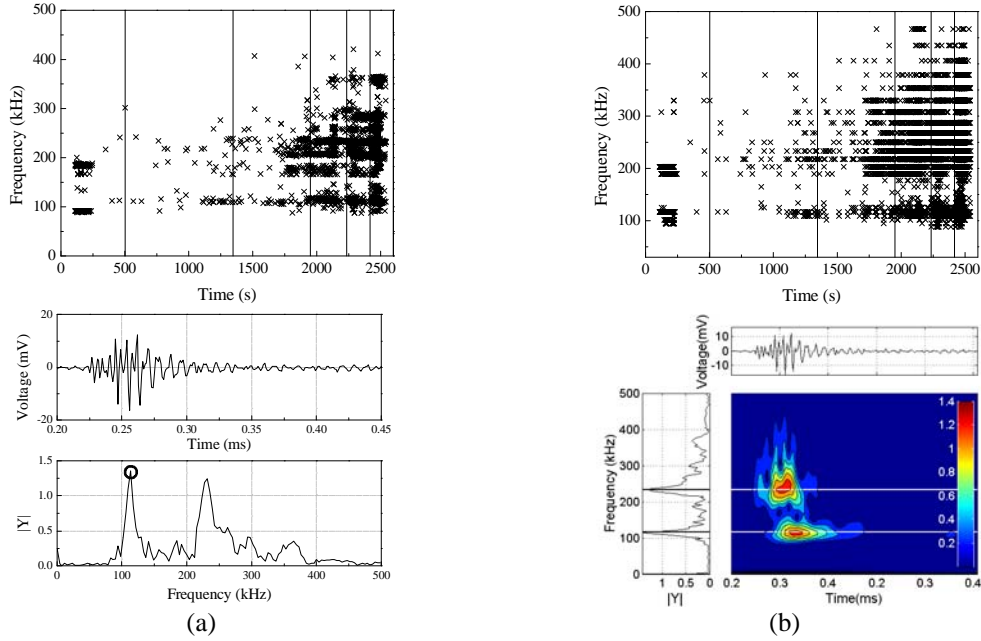Fig. 5 Frequency response in two kinds of AE signals

Fig. 6 Time frequency analysis of AE signals: (a) peak frequency method and (b) wavelet transform

Time-frequency analysis based on the wavelet transform is employed to analyze the multiple frequency components in this paper. The basic equations of the wavelet transform are briefly introduced as follows.

If there exists a function $\psi(t) \in L^2(R)$, and the following condition is satisfied

$$\int_{-\infty}^{\infty} \frac{|\Psi(\omega)|^2}{|\omega|} d\omega < \infty \tag{1}$$

where $\Psi(\omega)$ is the Fourier transform of $\psi(t)$.

$$\Psi(\omega) = \frac{1}{\sqrt{2\pi}} \int_{-\infty}^{\infty} \psi(t) e^{-i\omega t} dt \tag{2}$$

The function can be called a 'basic' or 'mother' wavelet with the condition given in Eq. (2). However, the mother wavelet is modified to another function through scaling and translation

$$\psi_{a,b}(t) = a^{-\frac{1}{2}} \psi\left(\frac{t-b}{a}\right) \qquad (a > 0, b \in R) \tag{3}$$

The wavelet coefficient of the signal $x(t) \in L^2(R)$ with the mother wavelet $\psi(t)$ at time a and scale b is

$$WT_x\left(a,b\right)=\left\langle x\left(t\right),\psi_{a,b}\left(t\right)\right\rangle=a^{-\frac{1}{2}}\int_{-\infty}^{\infty}x\left(t\right)\psi^*\left(\frac{t-b}{a}\right)dt$$

(4)

where a is the scale parameter, b is the location parameter, and the superscript * denotes complex conjugation.

Complex gauss 20 (cgau20) is proposed as the 'basic' wavelet in this paper. Then the multiple frequency components can be analyzed using the selected 'basic' wavelet. According to the previous study of AE phenomenon, the features of the AE signals (for instance, the frequency component and duration) are useful to determine the damage patterns of BFRP materials. As a comparison, the peak frequency method which picks the maximum frequency component of each AE signals is used in Fig. 6(a). However, the results of proposed method are shown in Fig. 6(b), which picks all the useful frequency components of AE signals. And we can obtain the detail information of the AE signal like this: this signal contains two different frequency components, one low frequency and one high frequency. The durations of different frequency components are not the same. The duration of the low frequency component is longer than the high frequency component. That may indicate the high frequency component represents much more brittle damage. And then, all the received signals have been analyzed, as shown in Fig. 6. Each point of the time-frequency graph represents an frequency component (energy peak) of the AE signal.

4. Fatigue damage evolution assessment based on the frequency distribution of the AE signal and SEM images

4.1 Results and discussions for the specimen of No. 1 (BFRP-1)

The time history of the AE signal during the entire loading process for the first specimen is shown in Fig. 7. The fatigue test for the first specimen lasts more than 2,500 sec (5,000 cycles). The time-frequency analysis of the AE signals from the fatigue test is illustrated in Fig. 8. Six loading stages are indicated by 5 lines in Figs. 7 and 8. The typical SEM pictures are shown in Fig. 9.
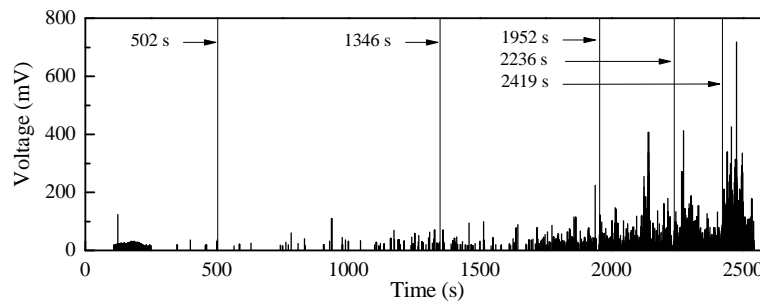

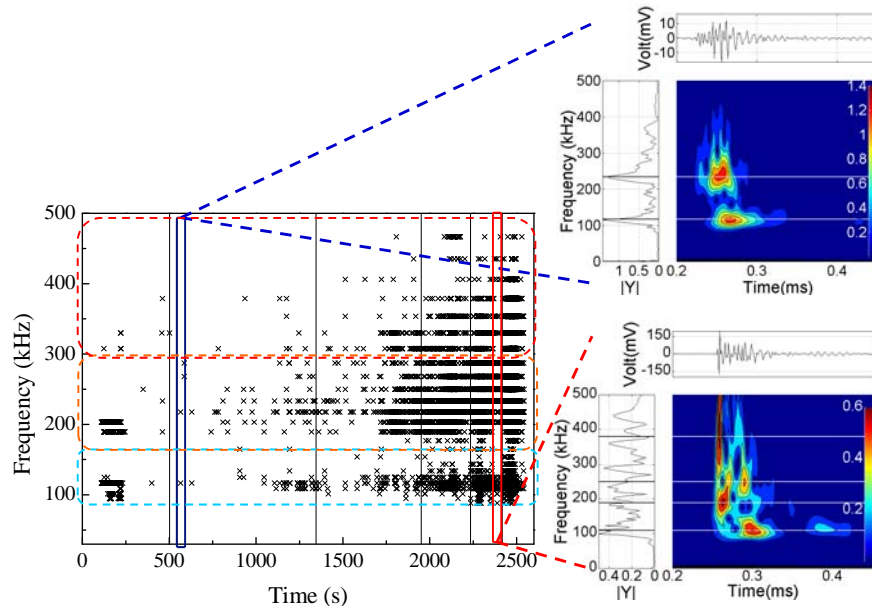Fig. 7 The amplitude vs. time-history graph for the BFRP-1 specimen

Fig. 8 Time-frequency analysis of AE signals using the wavelet transform

It can be seen from Fig. 7 that some AE events occur in the initial stage and the amplitudes of AE signals are not very high. The time-frequency graph (Fig. 8) shows that majority of the frequency components (energy peaks) are in the frequency ranges of 80-160 kHz and 200-300 kHz, which indicate most damage are matrix cracking and delamination.

At the end of this stage, several SEM pictures are obtained and shown in Fig. 9. It can be seen from Fig. 9 that one crack is clearly observed on the surface of the specimen. This crack starts from an initial defect point. Some white areas can be observed on the surface of the specimen because of the damaged matrix. No fractured fiber is found on the surface of specimen. Based on the above analysis of the AE signals, matrix cracking and delamination are the main damage patterns in the early stage.

In stage 2, only a few AE events occur (Fig. 7), and the corresponding frequencies are 100-300 kHz (Fig. 8). Therefore, the damage is still matrix cracking and delamination, while damage develops slowly.

According to the SEM pictures, there is no major damage in this stage. The specimen surface turns white, and the white areas extend significantly. The number of cracks increases.

In stage 3, AE signals clearly increase with the loading time. The time-frequency analysis indicates that not only the frequencies from 100 kHz to 300 kHz still exist, but the higher frequencies above 300 kHz also increase rapidly. Thus, a new type of damage may occur besides matrix cracking and delamination. Additionally, more AE events appear at the end of this stage, which implies that serious fatigue damage of the specimen begins.

From the SEM images of the third stage, the width of the cracks increase, and the damage of matrix is more severe. Additionally, some fractured fiber can be found in the SEM image. Therefore, it is reasonable to conclude that the high frequency component is related to the fiber fracture.
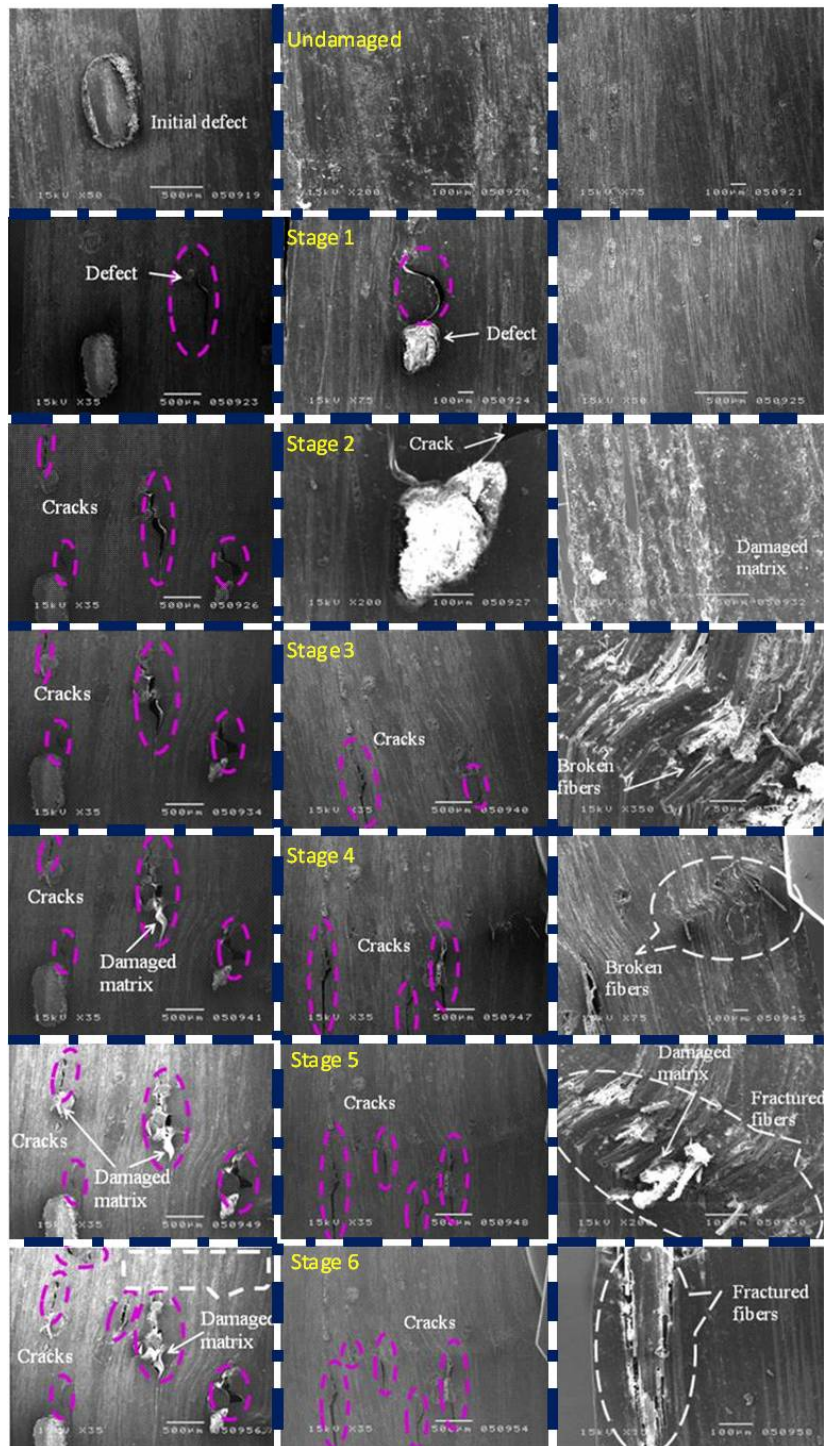
Fig. 9 Typical SEM images of the BFRP-1 specimen

It can be seen from Fig. 8 that the high frequency components continue to increase and some higher frequency components (higher than 400 kHz) occur in the stage. The number of AE events increases dramatically, and so many energy peaks are observed, which implies that fatigue damage becomes severe in this stage. Additionally, the broadening of frequency range is observed, which means lots of damage patterns occur in the BFRP specimen.

In this stage, the frequency in the range of 80-100 kHz is re-activated, and the AE events of the low frequency band increase quickly. At the end of this stage, some SEM images are obtained and shown in Fig. 9. From these SEM images, it is evident that the surface of the specimen gets much more white than before, which indicates the matrix damage release the low frequency energy peaks.

In the last stage of the fatigue test of the BFRP-1 specimen, more AE events appear, as shown in Fig. 8. The frequencies of AE signals contain all the possible frequencies, indicating that various damage patterns occur in the last stage.

Finally, it is seen from the SEM images shown in Fig. 9 that lots of cracks in various directions, and fractured fibers appear on the surface of BFRP specimen. The whole specimen surface totally gets white, indicating that the matrix is completely destroyed. Experimental results show that the fatigue damage types indicated by AE signals can be proved by SEM images well.

4.2 Results and discussions for the specimen of No. 1 (BFRP-2)

The fatigue test of the second BFRP specimen requires more than 7,000 sec (14,000 cycles). The curves of time history and time-frequency analysis of AE signal are shown in Figs. 10 and 11. Fig. 12 shows some typical SEM images.

The characteristics of stage 1 are similar to stage 2, the majority of the energy peaks are distributed from 100-300 kHz. However, the high frequency energy peaks occur at the beginning, which is different with the first specimen. The frequency characteristics in Fig. 11 imply that three basic damage patterns (matrix cracking, delamination and fibers fracture) occur at the beginning of the test. However, AE signals distribute sparsely in these two stages, which is the reason of the fatigue life of specimen-2 is longer than specimen-1.

From the SEM images (as shown in Fig. 12), it can be seen that there are two cracks on the surface of specimen-2. Some broken fibers and matrix damage are also observed, which is consistent with the AE signals.
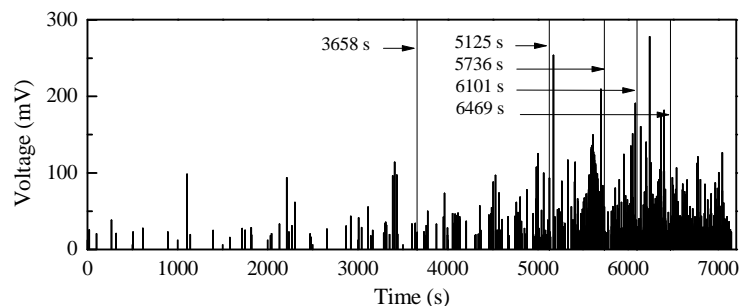

Fig. 10 The amplitude vs. time-history graph for the BFRP-2 specimen

For stages 3-6, the frequency bands of time-frequency analysis are similar. The number of AE events gradually increases, and the energy peak distribution becomes denser with time. In addition, high frequency components (higher than 400 kHz) appear, and the number of components increases in stages 4, 5 and 6, which indicates that lots of fibers break in these last three stages.

It can be seen from the SEM images shown in Fig. 12 that the numbers and widths of cracks increase with loading time. The matrix breaks into pieces (even powders), and many fractured fibers are also found on the surface of specimen.

The mechanical properties of BFRP specimens under static loading tests are stable that confirms the feasibility of hand lay-up method. However, the fatigue test of BFRP specimen-2 required more than 7,000 sec (14,000 cycles), which has a large difference with the fatigue life of the first specimen (2,500 sec, 5,000 cycles). Therefore, the difference should be attributed to the fatigue test is sensitive to initial defects.

5. Damage patterns and accumulated fatigue damage assessment

It can be seen from the wavelet transform graphs in Figs. 8 and 11 that there are three different frequency bands of AE signals in the entire fatigue test: low frequency (80-160 kHz), intermediate (160-300 kHz) and high frequency (above 300 kHz). According to previous studies in AE monitoring of FRP composites (de Groot *et al.* 1995, Ni and Iwamoto 2002), these three different frequency bands correspond to three basic damage patterns, that is, matrix cracking (low frequency band 80-160 kHz), delamination between the fiber and matrix (intermediate frequency band 160-300 kHz), and fiber fracture (high frequency band ≥ 300 kHz), as shown in Fig. 13.
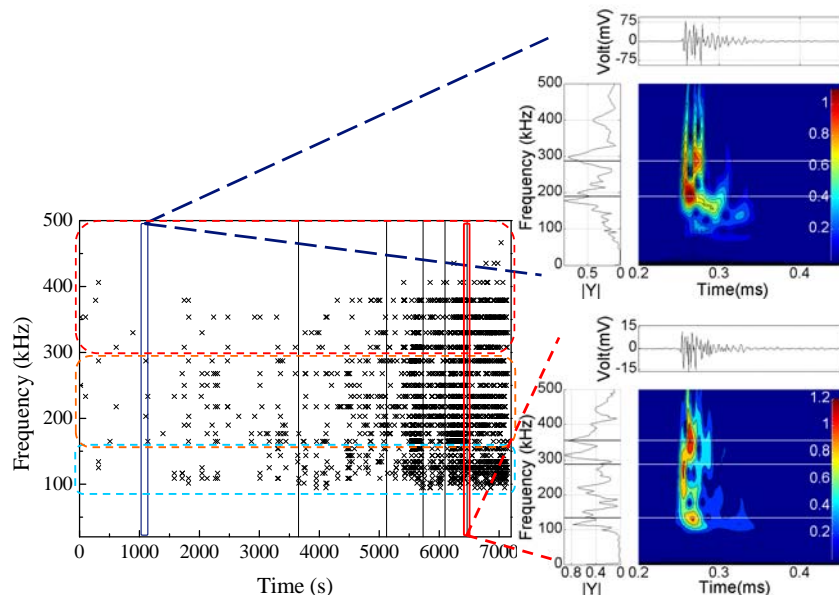

Fig. 11 Time-frequency analysis of the AE signals using the wavelet transform
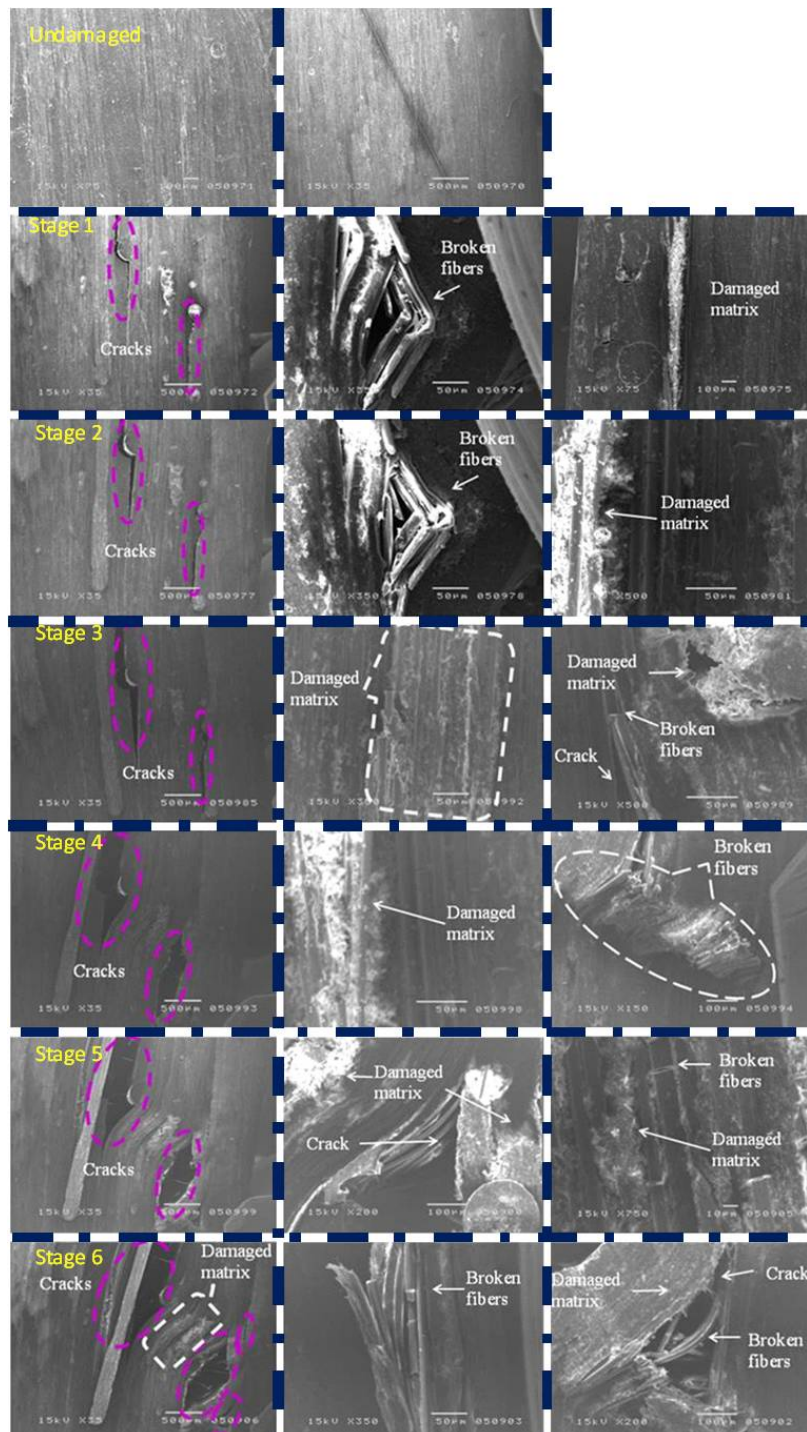
Fig. 12 The typical SEM images of BFRP-2 specimen

In this paper, we use BP1, BP2 and BP3 to represent these three basic damages. Actually, different basic damage patterns may occur in one damage event. Therefore, the damage patterns, based on the time-frequency analysis of AE signals, can be categorized into 7 groups, as listed in Table 2. The time-frequency graphs of the 7 different damage patterns are presented in Fig. 14.

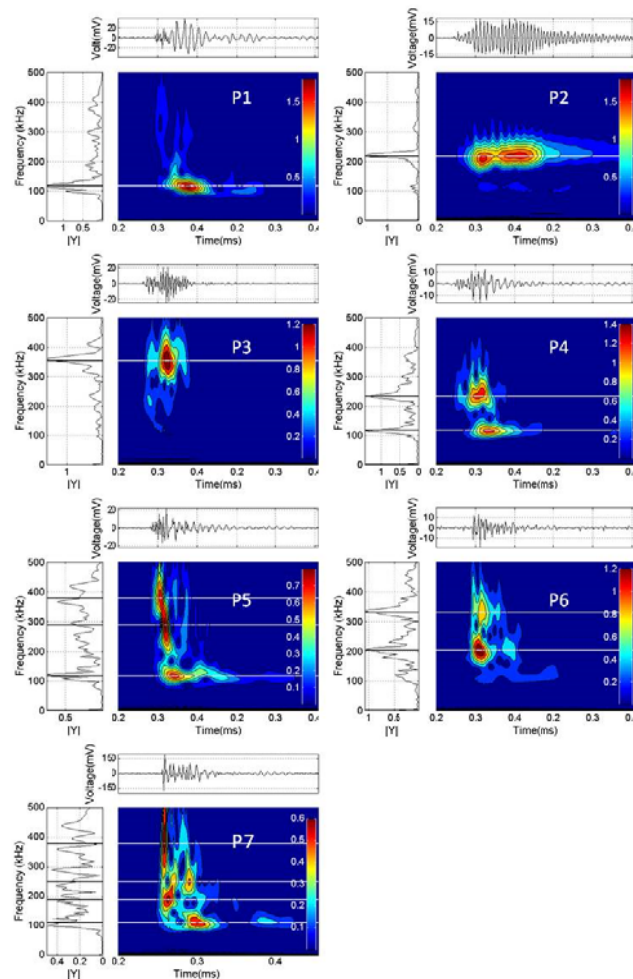Fig. 13 Three basic damage patterns of BFRP specimens

Fig. 14 Time-frequency graphs of 7 different damage patterns

Table 2 Damage patterns of BFRP specimens

Damage pattern	P1	P2	P3	P4	P5	P6	P7
Meaning	BP1	BP2	BP3	BP1+BP2	BP1+ BP3	BP2+ BP3	BP1+ BP2+ BP3

The released energy of the BFRP specimen during the fatigue test can be used as an indicator to evaluate the accumulated fatigue damage during the loading process. The energy can be calculated based on the wavelet coefficients, which is proposed to describe the accumulated fatigue damage. The cumulative energy from ω_1 to ω_2 can be defined as the integral of the 2-norm of the wavelet coefficients of the AE signal

$$E(t) = \int_0^t \int_{\omega_1}^{\omega_2} \left(WT_x \left(a(\omega), b \right) \right)^2 d\omega d\tau$$

(5)

The released energy of the AE signals of the two specimens is calculated by Eq. (5) and shown in Fig. 15. It can be seen from Fig. 15 that the released energy of the two specimens are very similar. Both of them increase very slowly at the beginning, while increase dramatically at the end. That represent a lot of the damage occurred at the end which is consistent with the experimental phenomenon. Furthermore, the released energy of low frequency bands is larger than high frequency band, and less than intermediate frequency. That may indicates that the delamination is the most important damage pattern in the fatigue damage of BFRP material.

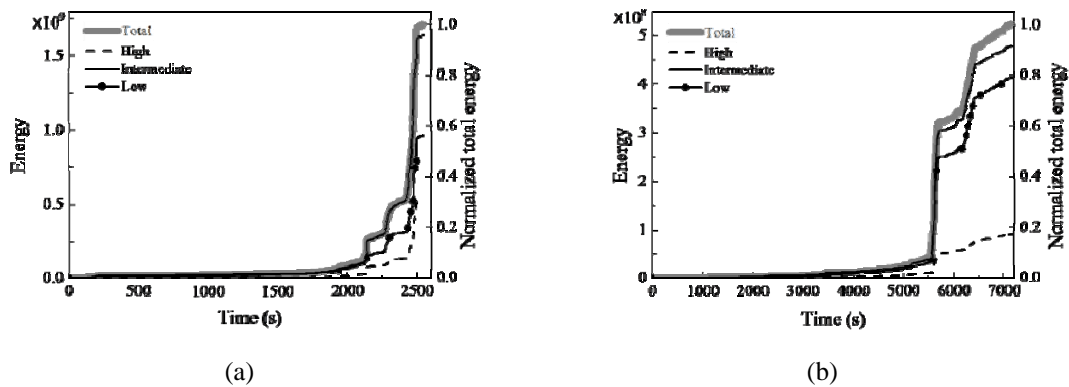(a)   (b)

Fig. 15 Cumulative energy evolution throughout the loading process: (a) BFRP-1 and (b) BFRP-2

The cumulative energy evolutions and number of various damage patterns of the two specimens are shown in Figs. 16 and 17, respectively. It can be seen from Fig. 16 that damage pattern 2 releases the most energy, which suggests that delamination dominates in the fatigue damage. Therefore, the bonding strength between fiber and matrix is one of the key factors of the bending strength of the BFRP specimen. It is worth noting that damage pattern P4 increases rapidly at the beginning of the fatigue test, which indicate the delamination play an important role in the early stage. The energy of damage patterns P6, P7, P1 and P4 are on the same order, which means that delamination with fiber fracture, matrix cracking with delamination and fiber fracture, matrix cracking, and matrix cracking with delamination release similar energy during the fatigue test. Damage patterns P3 and P5, especially damage pattern P5, release the smallest energy. That indicates fiber fracture and matrix cracking seldom occur together. Furthermore, we can conclude that fiber fracture may frequently cause delamination (P6 and P7). Matrix cracking and delamination can not only occur independently (P1, P2) but also induce each other (P4). Additionally, delamination and delamination coupled with matrix cracking occur at the beginning of the test, while fiber fracture always appears at the end of the test.

The cumulative energy of BFRP-2 is almost the same with that of BFRP-1. However, there are still some differences between them, as shown in Fig. 17. The damage pattern P4 is not such attractive in the early stage like BFRP-1. Matrix cracking, delamination and their combinations release the most energy, which is similar to the BFRP-1. That indicates the bonding between the matrix and fiber plays a key role in the fatigue life of BFRP material. Additionally, damage patterns P2 (delamination), P4 (matrix cracking coupled with delamination) and P5 (matrix cracking coupled with fiber fracture) release similar amounts of energy. Damage patterns P3, P6 and P7 which are all related to fiber fracture release the least amount of energy. Thus, it is concluded that fiber fracture is not so serious as matrix or delamination. Moreover, the little energy of P5 indicates that fiber fracture coupled with matrix cracking seldom occurs simultaneously, and the matrix damage is hard to cause the fiber fracture.
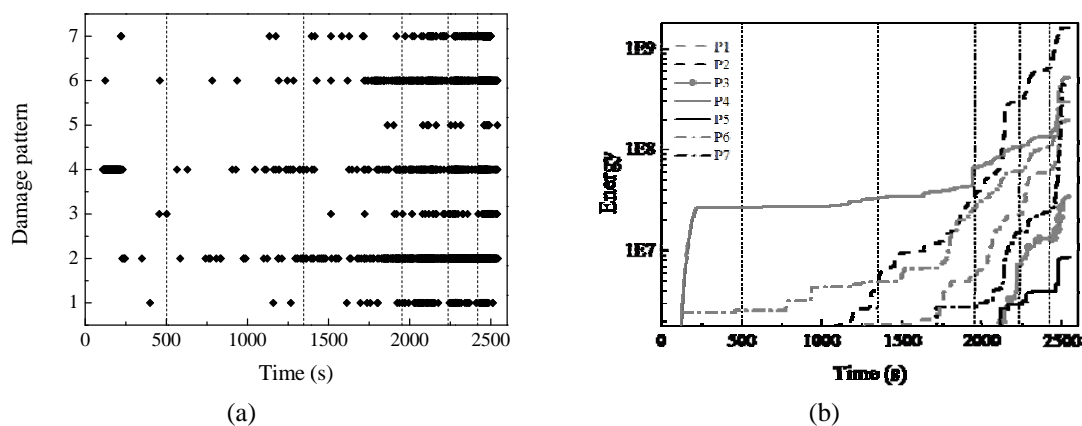

(a)

(b)

Fig. 16 Cumulative energy evolutions and number of various damage patterns for BFRP-1 during the fatigue test: (a) number and (b) released energy
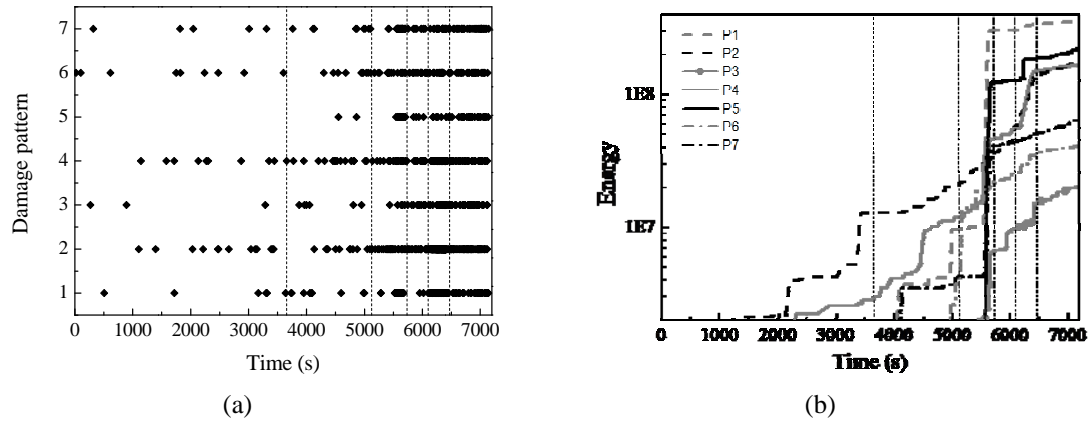
Fig. 17 Cumulative energy evolutions and number of various damage patterns for BFRP-2 during the fatigue test: (a) number and (b) released energy

6. Conclusions

In this paper, we focus on the damage mechanism, especially the different damage patterns of BFRP material. Therefore, the loading amplitude is to be appropriately designed to reduce the loading cycles and the loading time. Three-point bending fatigue tests are performed on BFRP plates, and the fatigue damage is monitored by the AE technique. Moreover, the SEM technique is employed to confirm the AE signals. The following conclusions are obtained:

• The feasibility of the hand lay-up method is confirmed through the static loading test. The results in terms of mechanical properties during static loading tests are repeatable and present low scatter. However, the loading cycles of two specimens under fatigue test have some difference. This difference in fatigue life of the two specimens indicates that the fatigue test is sensitive to initial defects.

• The time-frequency analysis method using wavelet transform is a good way to describe the features of acoustic emission signals. The AE signals of BFRP plates under fatigue test contain multiple components in the frequency response. The duration of high frequency component is shorter than the low one which presents the high frequency component may stand for more brittle damage pattern.

• Three main frequency bands of AE signals: low frequency band (80-160 kHz), intermediate frequency band (160-300 kHz) and high frequency band (above 300 kHz) are identified, which correspond to three different damage patterns: matrix cracking, delamination and fiber fracture, respectively. This result is confirmed by combining the SEM images and the time-frequency analysis.

• Three basic damage patterns which include matrix cracking, delamination, fiber fracture, and their combinations constitute all the 7 damage patterns of BFRP material. The cumulative energy of these three basic damage patterns during the fatigue tests can be obtained by calculating the wavelet coefficients. The cumulative energies of three basic damage patterns increase gradually with the number of loading cycles at the beginning, and increase

dramatically at the last stage of fatigue loading. Moreover, the cumulative energy of the three main frequency bands is intermediate frequency band > low frequency band > high frequency band. That indicates the delamination is the most serious damage pattern in FRP materials. Additionally, the energy of various damage patterns shows that fiber fracture usually occurs in the last loading stage. That implying the delamination usually causes the matrix damage at the beginning, while, with the increasing of loading time, the delamination induces fiber fracture at the end of fatigue test.

• The damage patterns which present fiber fracture and matrix cracking released the least energy. That declares fiber fracture and matrix cracking seldom occurs together, in other words, fiber fracture is not related to matrix cracking.

These results are very encouraging, but it should be pointed out that more specimens should be analyzed, and more AE parameters will be used to relate with the failure phenomena.

Acknowledgements

References

Caprino, G., Teti, R. and de Iorio, I. (2005), "Predicting residual strength of pre-fatigued glass fibre-reinforced plastic laminates through acoustic emission monitoring", *Compos. Part B - Eng.*, **36**(5), 365-371.

de Groot, P.J., Wijnen, P.A.M. and Janssen, R.B.F. (1995), "Real-time frequency determination of acoustic emission for different fracture mechanisms in carbon epoxy composites", *Compos. Sci. Technol.*, **55**(4), 405-412.

de Oliveira, R. and Marques, A.T. (2008), "Health monitoring of FRP using acoustic emission and artificial neural networks", *Comput. Struct.*, **86**(3-5), 367-373.

Ding, Y., Reuben, R.L. and Steel, J.A. (2004), "A new method for waveform analysis for estimating AE wave arrival times using wavelet decomposition", *NDT & E. Int.*, **37**(4), 279-290.

Eckles, W. and Awerbuch, J. (1988), "Monitoring acoustic-emission in cross-ply graphite epoxy laminates during fatigue loading", *J. Reinf. Plast. Comp.*, **7**(3), 265-283.

Fang, D. and Berkovits, A. (1995), "Fatigue design-model based on damage mechanisms revealed by acoustic-emission measurements", *J. Eng. Mater. - T ASME*, **117**(2), 200-208.

Giordano, M., Calabro, A., Esposito, C., D'Amore, A. and Nicolais, L. (1998), "An acoustic-emission characterization of the failure modes in polymer-composite materials", *Compos. Sci. Technol.*, **58**(12), 1923-1928.

Grabowska, J., Palacz, M. and Krawczuk, M. (2008), "Damage identification by wavelet analysis", *Mech. Syst. Signal Pr.*, **22**(7), 1623-1635.

Gutkin, R., Green, C.J., Vangrattanachai, S., Pinho, S.T., Robinson, P. and Curtis, P.T. (2011), "On acoustic emission for failure investigation in CFRP: Pattern recognition and peak frequency analyses", *Mech. Syst. Signal Pr.*, **25**(4), 1393-1407.

Maji, A.K., Satpathi, D. and Kratochvil, T. (1997), "Acoustic emission source location using lamb wave modes", *J. Eng. Mech. - ASCE*, **123**(2), 154-161.

Mizutani, Y., Nagashima, K., Takemoto, M. and Ono, K. (2000), "Fracture mechanism characterization of cross-ply carbon-fiber composites using acoustic emission analysis", *NDT & E. Int.*, **33**(2), 101-110.

Ni, Q.Q. and Iwamoto, M. (2002), "Wavelet transform of acoustic emission signals in failure of model composites", *Eng. Fract. Mech.,* **69**(6), 717-728.

Park, H.W., Sohn, H., Law, K.H. and Farrar, C.R. (2007), "Time reversal active sensing for health monitoring of a composite plate", *J. Sound Vib.*, **302**(1-2), 50-66.

Park, J.M., Kiin, P.G., Jang, J.H., Wang, Z., Hwang, B.S. and DeVries, K.L. (2008), "Interfacial evaluation and durability of modified Jute fibers/polypropylene (PP) composites using micromechanical test and acoustic emission", *Compos. Part B - Eng.*, **39**(6), 1042-1061.

Philippidis, T.P. and Assimakopoulou, T.T. (2008), "Using acoustic emission to assess shear strength degradation in FRP composites due to constant and variable amplitude fatigue loading", *Compos. Sci. Technol.*, **68**(3), 840-847.

Qi, G. (2000), "Wavelet-based AE characterization of composite materials", *NDT & E. Int.*, **33**(3), 133-144.

Sohn, H., Park, G., Wait, J.R., Limback, N.P. and Farrar, C.R. (2004), "Wavelet-based active sensing for delamination detection in composite structures", *Smart. Mater. Struct.*, **13**(1), 153-160.

Sung, D.U., Kim, C.G. and Hong, C.S. (2002), "Monitoring of impact damages in composite laminates using wavelet transform", *Compos. Part   B -Eng.*, **33**(1), 35-43.

Surgeon, M. and Wevers, M. (1999), "Modal analysis of acoustic emission signals from CFRP laminates", *NDT & E. Int.*, **32**(6), 311-322.

Unnthorsson, R., Runarsson, T. P. and Jonsson, M. T. (2008), "Acoustic emission based fatigue failure criterion for CFRP", *Int. J. Fatigue*, **30**(1), 11-20.

BF